Membrane Activity of the Peptide Antibiotic Clavanin and the Importance of Its Glycine Residues[†]

Ellen J. M. van Kan,*[,‡,§] Arie van der Bent,[‡] Rudy A. Demel,[§] and Ben de Kruijff[§]

Department of Industrial and Specialty Biochemicals, Renewable Resources, Agrotechnological Research Institute, Wageningen University and Research Centre, Bornsesteeg 59, 6708 PD Wageningen, The Netherlands, and Department of Biochemistry of Membranes, Centre for Biomembranes and Lipid Enzymology, Institute of Biomembranes, Utrecht University, Padualaan 8, 3584 CH Utrecht, The Netherlands

Received December 12, 2000; Revised Manuscript Received February 15, 2001

ABSTRACT: The peptide antibiotic clavanin A (VFQFLGKIIHHVGNFVHGFSHVF-NH_2) is rich in histidine and glycine residues. In this study the antimicrobial activity and membrane activity of wild-type clavanin A and seven Gly → Ala mutants thereof were investigated. Clavanin A effectively killed the test microorganism *Micrococcus flavus* and permeabilized its cytoplasmic membrane in the micromolar concentration range, suggesting that the membrane is the target for this molecule. Consistent with this suggestion, it was observed that clavanin A efficiently inserted into different phospholipid monolayers mainly via hydrophobic interactions. Bilayer permeabilization was observed for both low and high molecular mass fluorophores enclosed in unilamellar vesicles and occurred at the same concentration as the antimicrobial activity. It is therefore suggested that the loss of barrier function does not involve specific receptors in the target membrane. Circular dichroism spectroscopy indicated that under membrane mimicking conditions a random coil → helical transition was induced for all clavanin derivatives tested. Observed differences in peptide−membrane interaction and biological activity between the various clavanin derivatives demonstrated the functional importance of Gly at the positions 6 and 13. These two glycines may act as flexible hinges that facilitate the hydrophobic N-terminal end of clavanin to deeply insert into the bilayer. On the contrary, no such role is evident for Gly 18, as its substitution by Ala actually stimulated membrane interaction and biological activity. This study suggests that the combined hydrophobicity, overall state of charge, and conformational flexibility of the peptide determine the (membrane) activity of clavanin A and its Gly → Ala mutants.

During the past decade, interest in peptide antibiotics has tremendously increased. These peptides, which are widely distributed in nature and have been identified from many living species, take part in the innate defense against microbes (*1*−*4*). Although their primary sequences are highly heterogeneous, these peptides are generally often cationic and amphipathic. Their amphipathicity is enhanced upon the induction of specific secondary structures, such as α-helices, *β*-sheet structures which may be stabilized by disulfide bridges, or extended polyproline-like helices, and plays a key role in the antimicrobial mechanism of action. One of the main targets for these peptides is the lipid bilayer of the cytoplasmic membrane (*5*, *6*). Due to permeabilization of the membrane, the transmembrane potential is dissipated, and cell contents may be released, which finally result in cell death (*5*, *7*). The peptides exert this cell-lytic effect in two steps, i.e., initial binding to the cell surface, followed by membrane permeabilization (*7*).

Several mechanisms of membrane permeabilization are described in the literature. The membrane can be disturbed via the formation of transmembrane pores (*8*). Peptides may form pores according to the "barrel-stave" mechanism (*9*), which can act as ion-selective channels (*10*), or according to the toroidal model (*11*−*13*), in which dynamic peptide−lipid supramolecular complexes allow transbilayer transport of ions, lipids, and peptides. In a third model, membrane disruption occurs via a "carpet-like" mechanism in which the membrane surface is covered by peptides, resulting in structural collapse once a threshold concentration has been reached (*14*−*17*).

A few peptide antibiotics act via specific receptors in the cell membrane. The peptide nisin Z, for instance, uses the membrane-anchored cell wall precursor lipid II as a target molecule. Combined with its pore-forming ability, this high affinity for lipid II makes nisin a highly active compound (*18*).

Many natural antimicrobial peptides show selectivity for prokaryotic membranes over eukaryotic ones. This selectivity can be ascribed to differences in membrane composition and transmembrane potential which affect both the initial interaction and the permeabilization efficacy (*7*, *14*, *19*). Apart from these selectivity factors, peptide−membrane interactions are dependent on temperature, pH, and ionic strength (*6*, *13*).

[†] The study has been carried out with financial support from the Commission of the European Communities, Agriculture and Fisheries (FAIR) specific RTD program, CT97-3135.

* Corresponding author. Tel: +31 317 475328. Fax: +31 317 475347. E-mail: e.j.m.vankan@ato.wag-ur.nl.

[‡] Agrotechnological Research Institute.

[§] Utrecht University.

10.1021/bi0028136 CCC: $20.00
Published on Web 05/01/2001

A

GGG[a]	VFQFL**G**KIIHHV**G**NFVH**G**FSHVF-NH_2
AGG	VFQFL**A**KIIHHV**G**NFVH**G**FSHVF-NH_2
GAG	VFQFL**G**KIIHHV**A**NFVH**G**FSHVF-NH_2
GGA	VFQFL**G**KIIHHV**G**NFVH**A**FSHVF-NH_2
AAG	VFQFL**A**KIIHHV**A**NFVH**G**FSHVF-NH_2
AGA	VFQFL**A**KIIHHV**G**NFVH**A**FSHVF-NH_2
GAA	VFQFL**G**KIIHHV**A**NFVH**A**FSHVF-NH_2
AAA	VFQFL**A**KIIHHV**A**NFVH**A**FSHVF-NH_2

[a] wildtype Clavanin A sequence

B

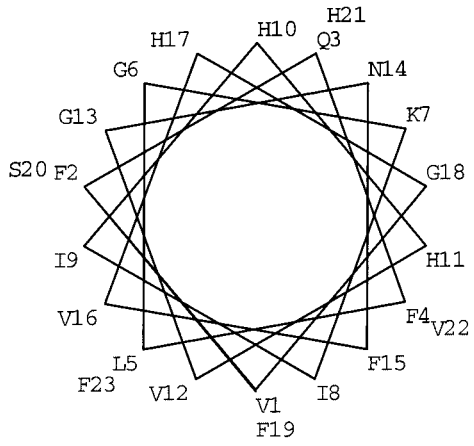

FIGURE 1: (A) Sequences of clavanin A and its alanine mutants. (B) Helical wheel representation of wild-type clavanin A.

One interesting class of antimicrobial peptides are the clavanins, which were isolated from the hemocytes of the tunicate *Styela clava* (*20*, *21*). Clavanin A (Figure 1A) contains 23 amino acid residues and can be folded into an amphipathic α-helix structure (*20*), as represented in Figure 1B. The clavanins display a particularly interesting amino acid composition. The presence of histidines could indicate a pH-dependent mode of action (*22*), as observed for the His-rich histatins (*23*), hisactophilin (*24*), and synthetic model peptides (*25*). The large number of hydrophobic valines and phenylalanines would argue for membrane affinity. As yet the mechanism of action of the clavanins remains unknown. Furthermore, the clavanins contain three glycine residues that are about evenly distributed along the peptide sequence. As glycines have poor helix-forming propensities, the question arises as to which role they play in the native sequence. To resolve both questions, the native clavanin A sequence and a series of seven Gly → Ala mutants (Figure 1A) were synthesized and examined for their antimicrobial and membrane activity. The monolayer technique was used to study peptide−lipid interactions during initial binding under varying conditions (*26*, *27*). Membrane permeabilization was analyzed via fluorescence spectroscopy using lipid bilayer systems and intact bacterial cells (*18*, *28*, *29*). Additionally, circular dichroism (CD)[1] spectroscopy was used to determine the peptide conformations in aqueous medium, structure-inducing solvents, and lipid vesicles (*10*). The results demonstrate that clavanin A exerts its antimicrobial activity by permeabilizing the membrane in which process the glycine residues play an important role.

EXPERIMENTAL PROCEDURES

Materials. *N*-α-Fmoc-protected amino acids, coupling reagent, and resin for peptide synthesis were obtained from Novabiochem (Läufelfingen, Switzerland). Solvents used for peptide synthesis and HPLC were purchased from Biosolve (Valkenswaard, The Netherlands). Mueller Hinton broth used as culture medium in the bacteriological assay was obtained from Oxoid (Unipath Ltd., Basingstoke, Hampshire, England). Membrane potential measurements were performed using the fluorescent dye 3,3′-diethylthiodicarbocyanine iodide [$DiSC_2(5)$] from Molecular Probes Inc. 1,2-Dioleoyl-*sn*-glycero-3-phosphoglycerol (DOPG), 1,2-dioleoyl-*sn*-glycero-3-phosphoethanolamine (DOPE), and 1,2-dioleoyl-*sn*-glycero-3-phosphocholine (DOPC) were purchased from Avanti Polar Lipids Inc, (Alabaster, AL). Carboxyfluorescein was purchased from Eastman Kodak Co. (Rochester, NY) and purified as described (*30*). Fluorescein isothiocyanate−dextran (FITC−dextran, average molecular mass 9400 Da) from Sigma Chemical (St. Louis, MO) was used. All other chemicals were of analytical or reagent grade.

Peptide Synthesis. Clavanin derivatives were synthesized by solid-phase peptide synthesis on an Abimed AMS 422 automated multiple peptide synthesizer (Langenfeld, Germany) using Fmoc (9-fluorenylmethoxycarbonyl) chemistry. The peptides were constructed on 25 μmol scale on a Rink amide MBHA resin to obtain derivatives having an amidated C-terminal end corresponding to the native clavanin A. PyBOP was used as activating reagent for sequential coupling of the amino acids. A double coupling procedure was used; each amino acid derivative was added in 5-fold molar excess. After completion of the sequence, cleavage from the resin and simultaneous side chain deprotection were achieved with a mixture of 90% TFA, 3% water, and 7% triisopropylsilane. Cold, dry methyl *tert*-butyl ether was used to precipitate the peptides. After lyophilization the peptides were stored at −20 °C. Peptide stock solutions (1 mg/mL) in 10 mM potassium phosphate buffer (pH 5.0) were prepared prior to the experiments.

Purification and Characterization of the Clavanin Mutants. Peptides were purified using reversed-phase high-performance liquid chromatography (RP-HPLC) on a Waters Symmetry C18 (19 mm × 300 mm, 100 Å pore size, 7 μm particle size) column (Milford, MA). As the mobile phase acetonitrile and water, both containing 0.05% TFA (v/v), were mixed in a linear gradient. Analytical RP-HPLC was used to check the peptides' purity on a Waters Symmetry

[1] Abbreviations: CD, circular dichroism; DMSO, dimethyl sulfoxide; DOPC, 1,2-dioleoyl-*sn*-glycero-3-phosphocholine; DOPE, 1,2-dioleoyl-*sn*-glycero-3-phosphoethanolamine; DOPG, 1,2-dioleoyl-*sn*-glycero-3-phosphoglycerol; ES-MS, electron spray mass spectrometry; Fmoc, 9-fluorenylmethoxycarbony; LUV, large unilamellar vesicle; MIC, minimal inhibitory concentration; SUV, small unilamellar vesicle; RP-HPLC, reversed-phase high-performance liquid chromatography; TFA, trifluoroacetic acid; TFE, trifluoroethanol.

C18 (3.9 mm × 150 mm, 100 Å pore size, 5 μm particle size) column. A 10−70% gradient of acetonitrile in water, both containing 0.05% TFA (v/v) in 60 min at a flow rate of 1 mL/min, was applied to assess peptide homogeneity (>95%). Molecular masses of the peptides were determined using electron spray mass spectrometry (ES-MS) to confirm their composition.

Antimicrobial Activity Determination. Minimal inhibitory concentration (MIC) values of the clavanin derivatives were determined in a growth inhibition assay against *Micrococcus flavus* (DSM 1790). In 96-well plates, peptides were diluted 2-fold serially in 50 μL of 10 mM potassium phosphate buffer (pH 7.0), starting from 500 μg/mL. Wells that did not contain any peptide material were used as growth control (100% growth). *M. flavus* cells were grown from an overnight culture in Mueller Hinton (MH) broth at 30 °C to mid-logarithmic phase. The bacterial cells were diluted to 3.2×10^5 cells/mL in 2 times concentrated MH broth, and 50 μL of this suspension was added to each well. The optical densities (OD) at 595 nm were measured after 30 min as a blank value (used for correction) and after 24 h incubation at 30 °C to determine the bacterial growth. The growth inhibition percentages, calculated as the ratio of corrected OD_{595nm} and OD_{595nm} of the growth controls, were plotted against the peptide concentration in growth inhibition curves.

Membrane Activity Assay. To test the effect of the peptides on the membrane integrity, the fluorescent membrane potential-sensitive probe 3,3′-diethylthiodicarbocyanine iodide [$DiSC_2(5)$] was used (*31*). *M. flavus* cells were grown at 30 °C to mid-logarithmic phase, harvested, washed once with buffer (150 mM NaCl, 10 mM potassium phosphate buffer, pH 7) at 4 °C, and resuspended in the same buffer and stored on ice to immediately start fluorescence measurements. Therefore, cells were added to a fluorescence cuvette at an OD_{600} of 0.035 together with 0.2 μM $DiSC_2(5)$. The fluorescence emission was monitored at 20 °C using a SPF 500C spectrofluorometer (SLM Instruments Inc.) at 670 nm (excitation of 650 nm). When the dye uptake was maximal, as indicated by a stable reduction in fluorescence due to quenching of the accumulated dye in the membrane interior, peptides were added to a 0.23 μM concentration. Full dissipation of the membrane potential was obtained using gramicidin D (to 0.2 nM concentration) solution from DMSO. The membrane potential dissipating activity of the peptides was expressed as the percent inhibition as follows:

$$\% \text{ inhibition} = 100[(F_p - F_0)/(F_g - F_0)]$$

in which F_0 is the stable fluorescence value after addition of the probe $DiSC_2(5)$, F_p is the fluorescence value 2 min after addition of the peptide, and F_g is the fluorescence value after addition of gramicidin D.

CD Spectroscopy. CD spectra were recorded on a Jasco-J600 spectropolarimeter in the range 190−260 nm using quartz cuvettes with a path length of 0.1 cm at room temperature. Five scans were averaged and corrected for the contributions of vesicles and solvents. The peptides were dissolved in either 10 mM potassium phosphate buffer (pH 5.0, 6.0, and 7.0) or TFE to obtain a final concentration of 0.25 mg/mL in the cuvette. Small unilamellar vesicles (SUVs) containing DOPG:DOPC (1:9) were prepared in 10 mM potassium phosphate buffer (pH 6.0) by sonication to reduce the influence of scattering at low wavelength. The peptide/lipid ratio was 1/25 (mol/mol) at a peptide concentration of 0.25 mg/mL.

CD spectral data have been analyzed and quantified using the deconvolution program CDNN based on neural network theory (*32*).

Monolayer Experiments. Monolayer surface pressure was measured by the (platinum) Wilhelmy plate method (*26*) at room temperature, using a Cahn D-202 microbalance. The subphase was continuously stirred with a magnetic bar. The peptides were added to the subphase through a hole in the edge of the Teflon dish. The dish had a volume of 5 mL and a surface area of 8.81 cm^2. Pressure changes were monitored until a maximal surface pressure increase was reached. The initial surface pressure of the lipid monolayer was 20 mN/m, unless indicated otherwise. The lipids were spread from a chloroform/methanol (2/1 v/v) solution. In the monolayer experiments 10 mM potassium phosphate buffers with different pH values were used as subphases. The standard deviations in the monolayer measurements were typically in the order of 5%.

Large Unilamellar Vesicle (LUV) Preparation. Dried DOPC films were hydrated with a 15 mM carboxyfluorescein or 10 mM FITC-labeled dextran solution at pH 7 to obtain a 20 mM lipid concentration. The lipid dispersions were subjected to 10 freeze−thaw cycles and subsequently extruded through 400 nm pore size polycarbonate filters as described (*33*). Nonentrapped carboxyfluorescein was removed by gel filtration on Sephadex G75 spin columns, and fluorescein labeled dextran on Sephacryl S300-HR, equilibrated with buffer containing 150 mM NaCl and 10 mM Tris at pH 7. The high-salt buffer had the same osmolarity as the enclosed carboxyfluorescein or dextran solution in order to prevent osmotic effects. The phospholipid content was determined as inorganic phosphate according to Rouser (*34*).

Leakage Experiments. Carboxyfluorescein or FITC−dextran loaded vesicles (16.5 μM on a phosphorus basis during measurements in the cuvette) were added to 1.2 mL of 150 mM NaCl and 10 mM Tris buffer, pH 7.0. The release of fluorescent dye initiated by addition of peptide solutions was monitored by measuring the fluorescence intensity at 515 or 517 nm for carboxyfluorescein or FITC−dextran, respectively (excitation 492 and 495 nm for CF or FITC−dextran, respectively) on a SPF 500 C spectrophotometer (SLM instruments Inc.) at 20 °C.

The release of fluorescent dye was calculated according to

$$R_f = 100[(F_t - F_0)/(F_{100} - F_0)]$$

where R_f is the fraction of dye released and F_0, F_t, and F_{100} are the fluorescence intensities at times $t = 0$, t, or after addition of 10 μL of 10% Triton X-100, respectively.

RESULTS

Peptide Synthesis and Characterization. Three glycine residues are found at positions 6, 13, and 18 of the wild-type clavanin A sequence (Figure 1A). The role of these glycines was studied by replacing these residues by alanines, which adapt α-helical conformations more readily. All

Table 1: Clavanin A Gly → Ala Mutants and Their Retention Time during RP-HPLC, Mass Spectral Data, and Antimicrobial and Membrane Activities against *M. flavus* (Strain DSM 1790)

peptide	retention time (min)	molecular mass (Da) measured	molecular mass (Da) expected	MIC value on *M. flavus* (μM)[a]	inhibition (%) of membrane potential on intact *M. flavus* cells[b,c] expt 1	inhibition (%) of membrane potential on intact *M. flavus* cells[b,c] expt 2
GGG (native)	33.3	2664.74	2664.43	4.9 ± 1.7	58	80
AGG	35.7	2678.64	2678.44	70 ± 33	27	50
GAG	37.3	2678.57	2678.44	5.8 ± 0.0	72	77
GGA	35.9	2678.55	2678.44	0.7 ± 0.0	104	103
AAG	39.8	2692.51	2692.46	>93	29	26
AGA	38.9	2692.58	2692.46	4.8 ± 1.7	102	76
GAA	40.1	2692.60	2692.46	1.4 ± 0.0	80	101
AAA	43.7	2706.58	2706.47	19 ± 7	44	35

[a] MIC values represent the average of three independent antimicrobial assays. [b] The effect of the peptides on the membrane potential of energized *M. flavus* cells was measured using the fluorescent dye $DiSC_2(5)$ as described in the Experimental Procedures section. [c] Membrane potential measurements were carried out twice; the inhibition percentages of the two independent measurements were depicted.

mono-, di-, and trisubstituted Gly → Ala derivatives of the C-terminally amidated native clavanin A sequence were synthesized. Analytical HPLC and ES-MS confirmed the purity and identity of the eight peptides that were purified using RP-HPLC (Table 1). Variations in retention behavior of the peptide mutants were observed. Retention times increased when glycines were mutated into alanines, reflecting increased hydrophobicities and possible conformational changes of the peptide analogues.

Antimicrobial Activity. The MIC values of the clavanin derivatives were determined against the Gram-positive species *M. flavus* in a growth inhibition assay (Table 1). Wild-type clavanin A (GGG) inhibited the bacterial growth of *M. flavus* at 5 μM. The peptides GGA and GAA were more potent than the native clavanin A and effectively inhibited growth at four to seven times lower concentrations. Peptides GAG and AGA displayed activity comparable to that of the wild-type peptide. Conversely, peptides AAA, AGG, and AAG were clearly less active against *M. flavus*. The differences in antimicrobial activity for the various clavanin derivatives emphasize the significance of the glycines at positions 6 and 13 of the clavanin sequence.

Membrane Activity Assay. As many antimicrobial peptides are assumed to kill the target microorganism via permeabilization of the plasma membrane, the effect of the clavanin derivatives on the membrane integrity of intact *M. flavus* cells was determined using the membrane potential-sensitive dye $DiSC_2(5)$. The fluorescence intensity of $DiSC_2(5)$, added at the first arrow in Figure 2, is strongly quenched when this dye accumulates in the membrane interior of energized cells. After a stable signal was observed, addition of the wild-type clavanin (trace 1) caused a rapid increase in fluorescence due to a collapse of the ion gradients which generate the membrane potential. Subsequent addition of gramicidin D, which fully collapses the membrane potential, only caused a small further increase in fluorescence, showing that clavanin A has almost completely permeabilized the membrane to small ions. Interestingly, the less potent antimicrobial peptide AAG showed a largely reduced ability to dissipate the membrane potential (trace 2).

The membrane potential-dissipating activities of clavanin A and all Gly → Ala derivatives are summarized in Table 1 and plotted against the MIC values in Figure 3. The peptides' abilities to disturb the membrane barrier function show a good correlation with the antimicrobial activities indicated

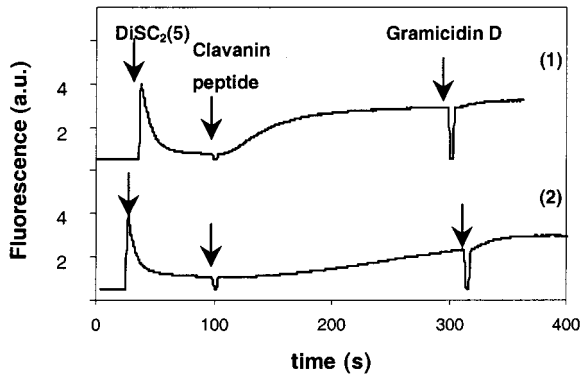

FIGURE 2: Effect of wild-type clavanin A (trace 1) and derivative AAG (trace 2) (peptide concentration 0.2 μM) on the membrane potential of intact *M. flavus* cells (OD_{600} = 0.035). The fluorescence of the membrane potential-sensitive dye $DiSC_2(5)$ was measured as described in the Experimental Procedures section.

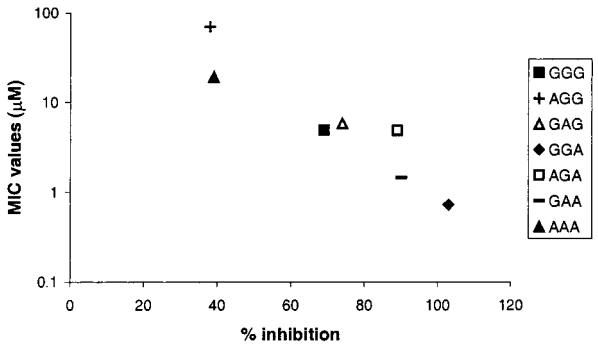

FIGURE 3: Inhibitory effects of the clavanin derivatives on the membrane potential of intact *M. flavus* cells vs their antimicrobial activity against this microorganism. The average percentages of membrane potential inhibition on *M. flavus* cells were depicted.

as MIC values. Both effects were observed in the same micromolar range of peptide concentration, strongly suggesting that the antibacterial activity of the peptides is due to permeabilization of the plasma membrane of the bacterial cell. To get more insight in the mode of action of the clavanins, secondary structure measurements were performed and model membrane systems were used to study the clavanin−membrane interactions.

CD Measurements. The secondary structure of the clavanin derivatives was analyzed by circular dichroism (CD) spectroscopy in aqueous solution, in TFE, and in the presence of SUVs. In aqueous solution, all peptide derivatives showed similar random coil spectra, as shown in Figure 4A (solid

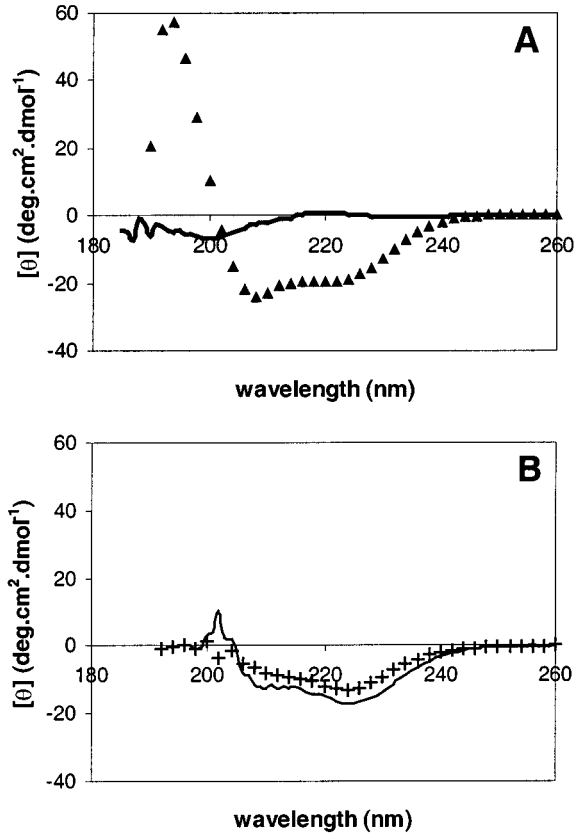

FIGURE 4: (A) CD spectra of wild-type clavanin A measured in 10 mM potassium phosphate buffer, pH 5.0 (continuous line), and in TFE (▲). (B) CD spectra recorded in the presence of DOPG:DOPC (1:9) SUVs in 10 mM potassium phosphate buffer, pH 6.0, for GGG (+) and AAA (continuous line).

line) for wild-type clavanin A. Deconvolution of the spectra obtained between pH 5 and pH 7 revealed that the peptide is mainly random coil in this pH range (41%, 47%, and 46% at pH 5, 6, and 7, respectively), with a low α-helix content of 10%, 5%, and 10% at pH 5, 6, and 7, respectively. In the structure-promoting solvent TFE all peptides display a typical α-helix spectrum (*35*), as observed in Figure 4A for the wild-type clavanin A. The calculated α-helix fractions were 71% for the native GGG and 77% for the AAA analogue, demonstrating that the glycine residues do not strongly interfere with helix formation in this solvent.

DOPG:DOPC (1:9) SUVs were used as stable model membrane systems to probe the vesicle−peptide interaction by CD. Figure 4B shows that the CD spectra of the wild-type peptide and the triple A mutant are also typical of an α-helical conformation, demonstrating the membrane affinity of these components. Analysis of these spectra resulted in 28% and 40% α-helix structure for the GGG and AAA peptides, respectively, suggesting that the degree of α-helicity induced by the membrane interaction was slightly enhanced upon the triple Gly to Ala mutation.

Monolayer Experiments. The initial interaction between peptides and bacterial membranes was studied using a phospholipid monolayer model system. Investigated parameters include the influence of the Gly → Ala mutations, peptide concentration, nature and packing of the phospholipids, and varying subphases (pH, salt concentration). A typical insertion experiment, represented in the insert in Figure 5, shows fast interaction of the wild-type clavanin A

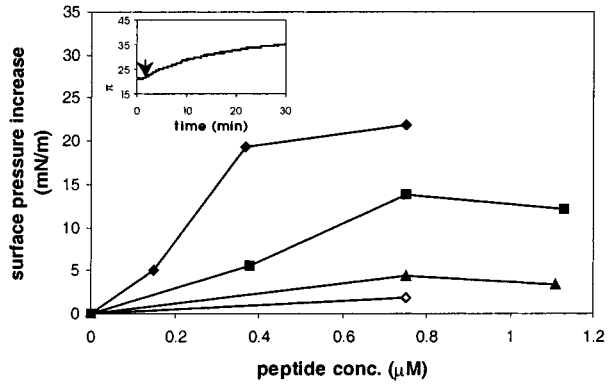

FIGURE 5: Typical insertion behavior of wild-type clavanin A (■) and mutants GGA (◆), AAA (▲), and AAG (◇) into DOPG:DOPE (1:3) lipid monolayers spread at 10 mM potassium phosphate buffer, pH 7.4. The initial surface pressure of the monolayer is 20 mN/m. The insert shows the kinetics of insertion of wild-type clavanin A (0.8 μM), indicated by the arrow, into a DOPG:DOPE (1:3) phospholipid monolayer spread at 10 mM potassium phosphate buffer, pH 7.4, with an initial surface pressure of 20 mN/m.

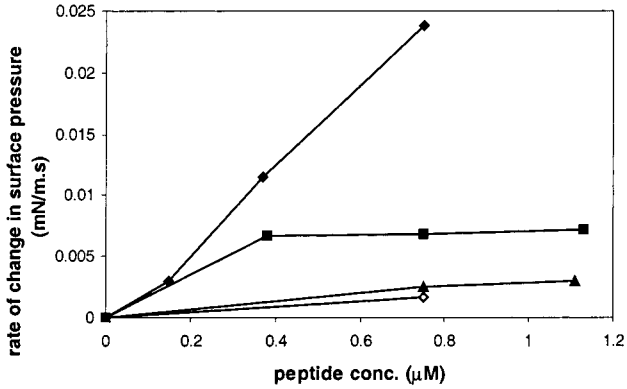

FIGURE 6: Kinetics of the insertion of wild-type clavanin A (■) and mutants GGA (◆), AAA (▲), and AAG (◇) into DOPG:DOPE (1:3) lipid monolayers spread at potassium phosphate buffer, pH 7.4. The initial surface pressure of the monolayer is 20 mN/m. The rate of change in surface pressures, determined as the initial tangents upon injection of the insertion process ($\Delta\pi$ over t curves) is plotted at the y-axis as a function of peptide concentration.

after injection in the aqueous subphase with the anionic DOPG:DOPE (1:3) lipid monolayer at the air/water interface. This composition was selected from its similarity to that of bacterial membranes. The degree of interaction with this lipid system is shown as the maximum surface pressure increase ($\Delta\pi$) of the monolayer. Depending on the applied conditions, maximal insertion is realized within 3−30 min for these peptides.

At a subphase pH of 7.4 wild-type clavanin A inserts efficiently into the monolayer, as shown by the large increase in surface pressure (Figure 5) and rate of insertion (Figure 6). Both parameters level off around a peptide concentration of 0.8 μM.

To examine the importance of the glycine residues for membrane insertion GGG and a subset of its Gly → Ala mutants were tested. GGA was chosen for its superior antimicrobial activity, whereas AAA and particularly AAG are less active than the wild-type clavanin (Table 1). At neutral pH, the maximal extent of monolayer insertion (Figure 5) correlates well with the MIC values and follows the order GGA > GGG > AAA > AAG. To some extent this is also reflected in the kinetics of insertion (Figure 6).

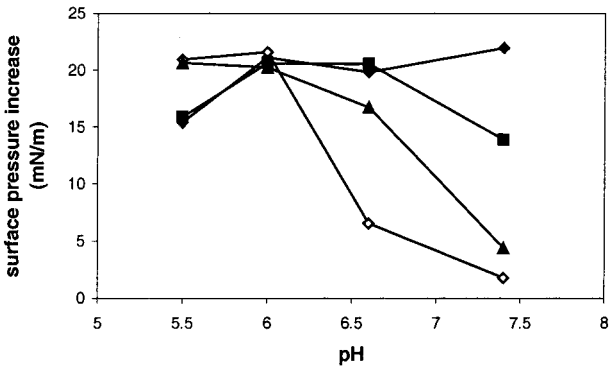

FIGURE 7: pH-dependent insertion of wild-type clavanin A (■) and mutants GGA (◆), AAA (▲), and AAG (◇) into DOPG:DOPE (1:3) lipid monolayers spread at 10 mM potassium phosphate buffer subphases. The peptide concentration in each measurement was 0.8 μM; π_i is 20 mN/m.

Clavanin A has four histidine residues with a pK_a of approximately 6. The charge of the peptide will therefore vary over the physiological pH range. To study the importance of the charge of the peptide on membrane interaction, monolayer insertion was analyzed between pH 5.5 and pH 7.5.

The insertion kinetics of clavanin A and the Gly → Ala mutants increased at pH 5.5 (data not shown), at which the peptide is most positively charged. For the wild-type peptide, however, the extent of insertion was only slightly pH dependent (Figure 7). This demonstrates that insertion is primarily driven by the hydrophobicity of clavanin. Whereas at lower pH all peptides show similar extents of insertion, differences in monolayer insertion occur at neutral pH. The potent GGA mutant showed behavior similar to that of native clavanin A; the less effective antimicrobial mutants AAA and AAG show a dramatically decreased insertion at the higher pH values. Also the mutants AGA and GAG which were comparably active as the wild-type compound in the bioassay showed reduced monolayer insertion above pH 7 (data not shown).

Since the DOPG:DOPE (1:3) monolayer is negatively charged, electrostatic interactions could possibly be involved in the clavanin−monolayer interaction at lower pH values. However, the pH-dependent insertion of clavanin A and the AAA mutant into a 100% DOPE monolayer was very similar to the mixed monolayer system (data not shown). The virtually identical insertion behavior for both of these monolayers and the similar results obtained at a higher ionic strength of 150 mM NaCl in the subphase (data not shown) underline the importance of the hydrophobic forces for insertion of the clavanin derivatives.

All results described so far were obtained with monolayers spread at an initial surface pressure of 20 mN/m. To gain an insight into the membrane penetration power of clavanin, the initial surface pressure was varied in the DOPG:DOPE (1:3) system. When π_i is increased, the packing density increases and, accordingly, insertion of the wild-type sequence decreases (Figure 8). Extrapolation of the data yields the exclusion pressure, defined as the pressure at which the peptide cannot penetrate into the monolayer. For the wild-type peptide values of 48 and 45 mN/m can be estimated at pH 5.5 and 7.4, respectively. This suggests that the peptide can insert at initial pressures in the physiological range of

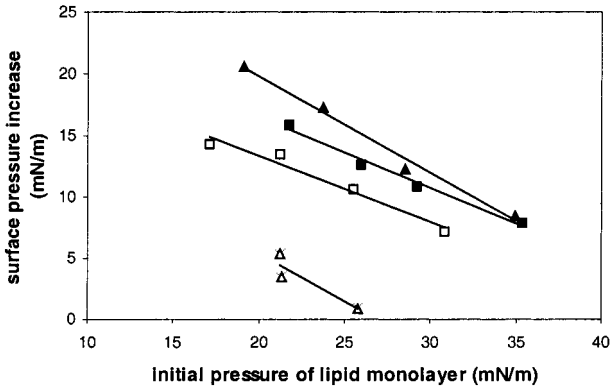

FIGURE 8: Penetration of wild-type clavanin A (squares) and the AAA variant (triangles) into DOPG:DOPE (1:3) lipid monolayers spread at 10 mM potassium phosphate buffer (pH 5.5, closed symbols, and pH 7.4, open symbols). Each measurement was performed by addition of 1 mg/mL peptide stocks underneath the monolayer to yield a concentration of approximately 0.8 μM.

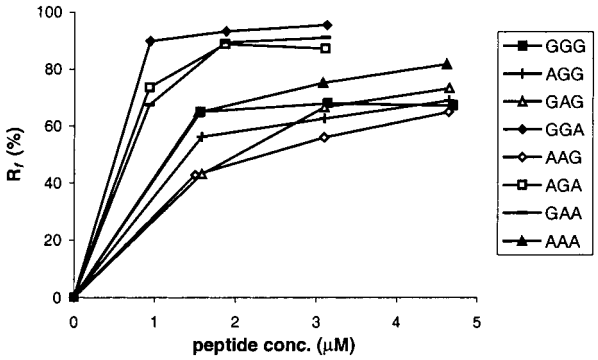

FIGURE 9: Release of the fluorescent probe carboxyfluorescein from DOPC LUVs at pH 7.0, measured 2 min after the addition of the peptides.

30−35 mN/m (*26*). At pH 7.4, the mutant peptide AAA cannot insert at these physiological pressures, which is consistent with its largely reduced antimicrobial activity. At the lower pH of 5.5 this peptide acquires a much stronger membrane penetration power and can insert up to pressures of 45 mN/m.

Permeabilization Experiments. LUVs of DOPC containing fluorescent probes were used as a model system to investigate whether the peptides affect the barrier function of the bilayer. LUVs of the DOPG:DOPE (3:7) phospholipid system, used in the monolayer experiments, had a highly unstable bilayer which was readily and nonspecifically perturbed by the peptides and therefore could not be used to test the specificity of the membrane permeabilization process. It was verified that the peptides inserted similarly into DOPC monolayers as in DOPG:DOPE (3:7) monolayers (data not shown).

At pH 7.0, wild-type GGG caused effective release of carboxyfluorescein from DOPC LUVs (Figure 9). The permeabilization occurs in the same concentration range as the monolayer insertion. The mutant peptides with increased antimicrobial activity, i.e., GGA and GAA, appear to permeabilize the DOPC LUVs more effectively. The mutants with decreased antimicrobial activity permeabilized the membrane to a comparable extent as the wild-type compound, despite their reduced monolayer insertion capacities.

To get more information about the membrane permeabilization mechanism, the high molecular mass probe FITC−dextran (9400 Da) was entrapped in DOPC vesicles. The

different clavanin peptides caused an efficient release of this high molecular mass FITC-labeled dextran with a comparable rate and peptide specificity as observed for the low molecular mass carboxyfluorescein (data not shown), suggesting a rather aspecific membrane permeabilization process.

DISCUSSION

In this study, the membrane interaction of clavanin A was investigated using intact cells and both monolayers and bilayers as model membranes. In addition, the role of the histidine and glycine residues therein was studied. The results demonstrate that clavanin A exerts its antibiotic activity by membrane permeabilization and points to an important role of the glycine residues in this process.

Addition of clavanin A to cell membranes of intact *M. flavus* cells resulted in dissipation of the membrane potential, due to the loss of vital ion gradients. Collapse of the membrane potential occurs at the same concentration as inhibition of growth of *M. flavus* cells, which strongly suggests that the membrane is the target of the clavanins. In accordance, wild-type clavanin A was found to insert with high affinity into different lipid monolayer systems in a concentration-dependent manner and with a high initial rate. Penetration experiments showed that clavanin A can readily insert at initial surface pressures near the physiological range of 30−35 mN/m (*26*), at both pH 5.5 and pH 7.4 in accordance with the membrane permeabilizing process. Whereas when the pH was increased the insertion rate was reduced, the maximal extent of monolayer insertion of clavanin A hardly depended on the pH in the range between 5.5 and 7.4. Considering this pH independence and the essentially identical insertion behavior into both negatively charged and neutral phospholipid monolayers, the actual monolayer insertion of clavanin A appears to be dominated by hydrophobic forces, thus indicating that the state of charge of the histidines does not play a major role in the peptide−lipid interactions. These histidines may have alternative functions, such as binding of cations and/or DNA and RNA macromolecules (*36*, *37*) (E. van Kan et al., unpublished results).

Interaction of clavanin A with lipid bilayers resulted in permeabilization, as measured by the similar release of both low and high molecular mass fluorescent dyes from DOPC LUVs. A nonspecific membrane permeabilization mechanism, such as the carpet model described by Shai (*14*), is therefore more plausible than more specific mechanisms that involve pores that, due to their limited sizes, do not allow the passage of high molecular mass probes (*8*, *13*).

As clavanin A is active in the micromolar range in both the bioassays and the various membrane model systems, it is unlikely that this peptide acts via specific receptors (*38*).

In the bioassay, considerable differences in antimicrobial activity against the testorganism *M. flavus* were observed for clavanin A and its Gly → Ala derivatives. GAA and, particularly, GGA were more potent antimicrobial agents than the wild-type clavanin A. The growth inhibition correlated well with the peptides' ability to permeabilize the cell membrane, as measured after addition of these peptides to intact *M. flavus* cells in the presence of the membrane potential-sensitive probe $DiSC_2(5)$.

The observed variations in membrane activity and bioactivity of clavanin A and the Gly → Ala derivatives, which were consistent with their monolayer insertion behavior at neutral pH, therefore, seem to result from specific Gly → Ala substitutions which may affect the peptides' conformation flexibility. The glycine residues at the positions 6 and 13, in this respect, appear to be important for a productive membrane interaction. At low pH, all clavanin derivatives show the same high extent of insertion into the DOPG:DOPE (1:3) monolayer. This efficient monolayer insertion of these highly charged (+6, 1K, 4H and N-terminus) compounds suggests that the peptide flexibility is less important.

No complete correlation could be observed between the permeabilization experiments using LUVs and the insertion into monolayers and activities against bacterial systems. This may be due to differences in membrane architecture between the model bilayers and natural cell membranes. Nevertheless, the most potent antimicrobial peptides, which showed the most pronounced insertion into lipid monolayers, also caused the most efficient release of fluorophores from lipid vesicles.

What could be the molecular interpretation of the effects observed for the different Gly → Ala substitutions? When Gly residues are mutated into alanines, the overall hydrophobicity of the peptide increases. Not all Gly → Ala substitutions, however, affect the membrane interaction to the same extent. In addition, the retention times of the peptides during RP-HPLC increased for the Ala mutants depending on the mutation site (Table 1). Both observations suggest that the Gly → Ala mutations also have an impact on the overall conformation of the peptide.

In accordance with this hypothesis, an increase in α-helix degree was measured using CD in the presence of DOPG:DOPC (1:9) vesicles going from the wild-type clavanin to the triple Ala mutant.

The glycine residue at position 6 appears to be essential for high bioactivity. The presence of the N-terminal glycine may give the peptides some flexibility, which seems advantageous for insertion into the phospholipid monolayer. The N-terminal segment preceding the first glycine of the clavanins is highly hydrophobic and contains no cationic residues. Possibly, the glycine at position 6 facilitates this part of the peptide to insert more deeply into the membrane bilayer and, therewith, to more drastically disturb the membrane. The peptide segment aligned by glycines 6 and 13 forms a perfect amphipathic structure when folded into a helix and contains one lysine residue, which may interact with the phospholipid headgroup region with high affinity (39).

Mutation of the glycine at position 18, at the C-terminal end, to alanine seems to favor the activity of the peptides compared to the wild type. Replacement of this glycine enables the C-terminal part of the peptide, starting from residue 14, to form a single, elongated amphipathic α-helical segment, which can lie parallel to the membrane. This orientation will be promoted by the three phenylalanines, which are located on the same face of this C-terminal part of the peptide in the helical state. These aromatic amino acids are interface-seeking residues, which may act as anchoring sites in the membrane interface region (*40*).

Overall, the picture emerges that the glycines form hinges between the various α-helical segments, which are stabilized on the membrane interface by the presence of phenylalanines and a lysine, thus promoting conformational flexibility. Whether this flexibility results in increased activities of the

clavanins depends on the position of the glycines. Apparently, the driving force to interact with the membrane and the required flexibility are most optimally combined in the most potent peptide, GGA, as expressed in the capacity to destabilize natural and model membranes.

ACKNOWLEDGMENT

The authors thank Kees Versluis, Department of Biomolecular Mass Spectrometry, Utrecht University, for doing the electrospray mass spectrometry measurements.

REFERENCES

1. Boman, H. G. (1998) *Scand. J. Immunol. 48*, 15−25.
2. Nissen-Meyer, J., and Nes, I. F. (1997) *Arch. Microbiol. 167*, 67−77.
3. Lehrer, R. I., and Ganz, T. (1996) *Ann. N.Y. Acad. Sci. 797*, 228−239.
4. Gudmundsson, G. H., and Agerberth, B. (1999) *J. Immunol. Methods 232*, 45−54.
5. Epand, R. M., and Vogel, H. J. (1999) *Biochim. Biophys. Acta 1462*, 11−28.
6. Blondelle, S. E., Lohner, K., and Aguilar, M.-I. (1999) *Biochim. Biophys. Acta 1462*, 89−108.
7. Dathe, M., and Wieprecht, T. (1999) *Biochim. Biophys. Acta 1462*, 71−87.
8. Huang, H. W. (2000) *Biochemistry 39*, 8347−8352.
9. He, K., Ludtke, S. J., Worcester, D. L., and Huang, H. W. (1996) *Biophys. J. 70*, 2659−2666.
10. Sitaram, N., and Nagaraj, R. (1999) *Biochim. Biophys. Acta 1462*, 29−54.
11. Ludtke, S., Heller, W. T., Harroun, T. A., Yang, L., and Huang, H. W. (1996) *Biochemistry 35*, 13723−13728.
12. Matsuzaki, K., Murase, O., Fujii, N., and Miyajima, K. (1996) *Biochemistry 35*, 11361−11368.
13. Matsuzaki, K. (1999) *Biochim. Biophys. Acta 1462*, 1−10.
14. Shai, Y. (1999) *Biochim. Biophys. Acta 1462*, 55−72.
15. Shai, Y., and Oren, Z. (1996) *J. Biol. Chem. 271*, 7305−7308.
16. Gazit, E., Boman, H. G., and Shai, Y. (1995) *Biochemistry 34*, 11479−11488.
17. Oren, Z., and Shai, Y. (1999) *Biopolymers 47*, 451−463.
18. Breukink, E., Wiedemann, I., Van Kraaij, C., Kuipers, O. P., Sahl, H.-G., and De Kruijff, B. (1999) *Science 286*, 2361−2364.
19. Vaara, M. (1992) *Microbiol. Rev. 56*, 395−411.
20. Lee, I. H., Zhao, C., Cho, Y., Harwig, S. S. L., Cooper, E. L., and Lehrer, R. I. (1997) *FEBS Lett.* 158−162.
21. Zhao, C., Liaw, L., Lee, I. H., and Lehrer, R. I. (1997) *FEBS Lett. 410*, 490−492.
22. Lee, I. H., Cho, Y., and Lehrer, R. I. (1997) *Infect. Immun. 65*, 2898−2903.
23. Xu, T., Levitz, S. M., Diamond, R. D., and Oppenheim, F. G. (1991) *Infect. Immun. 59*, 2549−2554.
24. Hanakam, F., Gerisch, G., Lotz, S., Alt, T., and Seelig, A. (1996) *Biochemistry 35*, 11036−11044.
25. Vogt, T. C. B., and Bechinger, B. (1999) *J. Biol. Chem. 274*, 29115−29121.
26. Demel, R. A. (1994) in *Subcellular Biochemistry* (Hilderson, H. J., and Ralston, G. B., Eds.) pp 83−120, Plenum Press, New York.
27. Maget-Dana, R. (1999) *Biochim. Biophys. Acta 1462*, 109−140.
28. Breukink, E., Van Kraaij, C., Demel, R. A., Siezen, R. J., Kuipers, O. P., and De Kruijff, B. (1997) *Biochemistry 36*, 6968−6976.
29. Driessen, A. J. M., Van den Hooven, H. W., Kuiper, W., Van de Kamp, M., Sahl, H.-G., Konings, R. N. H., and Konings, W. N. (1995) *Biochemistry 34*, 1606−1614.
30. Weinstein, J. N., Ralston, E., Leserman, L. D., Klausner, R. D., Dragsten, P., Henkart, P., and Blumenthal, R. (1984) in *Liposome Technology* (Gregoriadis, G., Ed.) p 183, CRC Press, Boca Raton, FL.
31. Sims, P. J., Waggoner, A. S., Wang, C. H., and Hoffmann, J. R. (1974) *Biochemistry 13*, 3315−3330.
32. Böhm, G., Muhr, R., and Jaenicke, R. (1992) *Protein Eng. 5*, 191−195.
33. Hope, M. J., Bally, M. B., Webb, G., and Cullis, P. R. (1985) *Biochim. et Biophys. Acta 812*, 55−62.
34. Rouser, G., Fleischer, S., and Yamamoto, A. (1970) *Lipids 5*, 494−496.
35. Chen, Y. H., Yang, J. T., and Martinez, H. M. (1972) *Biochemistry 11*, 4120−4131.
36. Melino, S., Rufini, S., Sette, M., Morero, R., Grottesi, A., Paci, M., and Petruzzelli, R. (1999) *Biochemistry 38*, 9626−9633.
37. Morcock, D. R., Sowder, R. C., and Casas-Finet, J. R. (2000) *FEBS Lett. 476*, 190−193.
38. Breukink, E., and De Kruijff, B. (1999) *Biochim. Biophys. Acta 1462*, 223−234.
39. De Planque, M. R. R., Kruijtzer, J. A. W., Liskamp, R. M. J., Marsh, D., Greathouse, D. V., Koeppe, R. E., De Kruijff, B., and Killian, J. A. (1999) *J. Biol. Chem. 274*, 20839−20846.
40. Wimley, W. C., and White, S. H. (1996) *Nat. Struct. Biol. 3*, 842−848.

BI0028136